Adv Polym Sci (2006) 195: 177–210
DOI 10.1007/12_051

Published online: 15 November 2005

Water Solutions of Amphiphilic Polymers: Nanostructure Formation and Possibilities for Catalysis

Ivan M. Okhapkin[1,2] · Elena E. Makhaeva[1] · Alexei R. Khokhlov[1,2,3] (✉)

[1]Department of Polymer Science, University of Ulm, Albert-Einstein-Allee 11, 89069 Ulm, Germany
khokhlov@polly.phys.msu.ru

[2]Nesmeyanov Institute of Organoelement Compounds, Vavilov Street 28, 119991 Moscow, Russia
khokhlov@polly.phys.msu.ru

[3]Physics Department, Moscow State University, 119992 Moscow, Russia
khokhlov@polly.phys.msu.ru

Abstract A concept of amphiphilicity in application to monomer units of water-soluble polymers is presented. Molecular simulation and experimental studies of polymers consisting of amphiphilic monomers units are reviewed. Those polymers reveal unusual conformational behavior in aqueous solutions forming nanostructures of nonspherical shape. Self-association of amphiphilic thermosensitive polymers in water solutions is discussed. Possibilities for the use of thermosensitive copolymers as catalysts are described. The sharp water–organic boundaries formed by polymer associates in water solutions are shown to be a prospective medium for catalysis owing to adsorption of interfacially active substrates at the interface.

Keywords Amphiphilic monomers · Interfaces · Polymer catalysts · Water-soluble polymers

Abbreviations

CAC	Critical aggregation concentration
EO	Ethylene oxide
LCST	Lower critical solution temperature
MAA	Methacrylic acid
MMA	Methyl methacrylate

NIPA	*N*-Isopropylacrylamide
NPA	*p*-Nitrophenyl acetate
NPAlk	*p*-Nitrophenyl alkanoates
PDEVP	Poly(*N*-(*n*-dodecyl)-4-vinylpyridinium-*co*-*N*-ethyl-4-vinylpyridinium) bromide
PEO	Poly(ethylene oxide)
PFDA	Perfluorododecanoic acid
PNIPA	Poly(*N*-isopropylacrylamide)
PS	Polystyrene
PVCL	Poly(*N*-vinylcaprolactam)
PVim	Poly(1-vinylimidazole)
R_g	Radius of gyration
R_h	Hydrodynamic radius
SAXS	Small-angle X-ray scattering
SMTBA	Styrylmethyl(tributyl)ammonium
SMTMA	Styrylmethyl(trimethyl)ammonium
SMTMAC	Styrylmethyl(trimethyl)ammonium chloride
TEM	Transmission electron microscopy
Tris	Tris(hydroxymethyl)aminomethane
VCL	*N*-Vinylcaprolactam
Vim	1-Vinylimidazole
VP	*N*-Vinylpyrrolidone

1 Introduction

Development of systems based on water-soluble polymers is one of the main research tasks of polymer chemistry and physics, since for natural macromolecules, such as proteins and DNA, water is the basic good solvent. In the last few decades, synthetic water-soluble polymers have found wide use in various biomedical applications [1–6] and separation processes [7–12]. Choosing water as a solvent is logical in many areas of research, such as biomedical applications and design of nanosize objects. Normally, nanosized objects are characterized by relatively high interfacial energy owing to their extremely small sizes. Water is an optimal medium for development of those objects. On the one hand, it possesses high interfacial tension at the boundaries with numerous compounds, which makes their molecular dissolution impossible. On the other hand, there are methods (e.g., addition of surfactants) that allow stabilization of the newly formed structures from macrophase separation. Water-soluble polymers are indeed prospective materials for this task. The intrinsic amphiphilic character enables them both to form nanosized structures and to stabilize the systems which are prone to macrophase separation.

Catalysis is a relatively new area for application of water-soluble polymers. Normally, organic solvents are conventional media for catalytic reactions. In recent years significant progress in the design of water-soluble catalysts was

achieved [13–15], as water appears a prospective environmentally friendly solvent for "green" chemistry purposes. Also, a number studies were carried out that used biomimetic approaches for construction of synthetic macromolecular enzyme models [16–18]. Water is often used for that task as it is the native medium for enzymes.

Globular proteins (including enzymes) form an important class of water-soluble natural polymers. Their globular structure is believed to be stabilized by hydrophobic interactions. Indeed, a protein globule consists of a hydrophobic core and a hydrophilic shell interacting with the solvent molecules and preventing them from having contact with the core (Fig. 1) [19]. Owing to such structural organization, protein globules are stable against aggregation in solutions. Furthermore, protein folding is also ruled by the balance of hydrophobic and hydrophilic interactions. The approach of treating protein folding and stability in binary terms of hydrophilicity and hydrophobicity is rather simplistic but it has an advantage of employing few parameters and approximations with reasonable results obtained on conformational behavior of proteins. This approach was found to be promising in application to synthetic polymers as well. The initial works in this field were those of Lau and Dill [20, 21], who proposed the subdivision of synthetic monomer units into "hydrophobic" and "polar" classes (HP model). Within this model, an amphiphilic macromolecule is considered as a chain in which hydrophobic and polar units are taken to be pointlike interaction sites distributed along the chain in a linear fashion (Fig. 2a). It is assumed that in water and other polar solvents the hydrophilic groups are in good-solvent conditions, while the hydrophobic groups are in poor-solvent conditions, so that the hydrophobic units attract each other, while the interaction between polar units is effectively repulsive.

However, normally, the groups of both types are present in synthetic and natural monomer units of water-soluble polymers (Scheme 2), which suggests that the units are amphiphilic rather than hydrophobic or hydrophilic. Vasilevskaya et al. [22, 23] reported a dumbbell model of the monomer unit in a chain in which a new representation of monomer units was proposed. In this representation, the amphiphilic character of the monomer units was

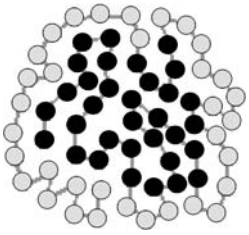

Fig. 1 Schematic representation of spatial structure of globular proteins. *Dark* and *light circles* denote hydrophobic and hydrophilic monomer units, respectively

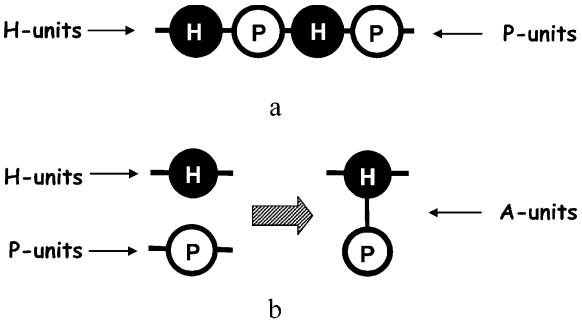

Fig. 2 Schematic representation of **a** the HP model and **b** the dumbbell HA model of an amphiphilic copolymer. *P-units* are hydrophilic (polar), *H-units* are hydrophobic, and *A-units* are amphiphilic. (Adapted from Ref. [25])

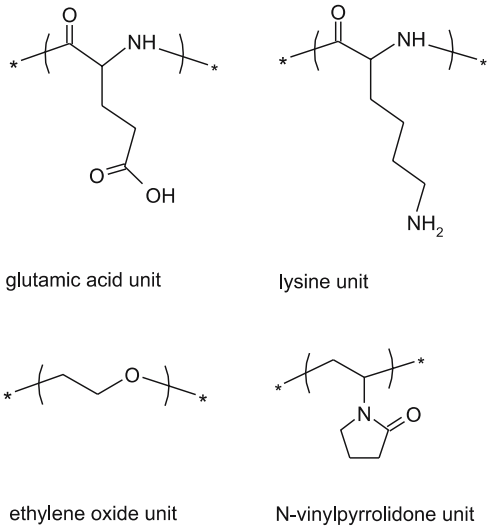

Scheme 1 Amphiphilic monomer units of synthetic and natural polymers

taken into account: the monomer unit was taken to consist of two parts, namely, a hydrophobic node of backbone and a polar segment attached to the node as a side group. In such a model, conformational properties of polymers, especially in the globular state, were shown to be drastically different from those predicted by the HP model and this prediction was supported by independent experimental results.

The present review has the following structure. In Sect. 2, the properties of amphiphilic monomers are discussed and a special classification of monomer units according to interfacial and partition properties is described. Also, the possibility of nanostructure formation in polymers composed of amphiphilic monomers is touched upon. This topic is more broadly treated in Sect. 3, where conformational properties of a key class of water-soluble polymers are

discussed, i.e., thermosensitive polymers. In Sect. 4, catalytic effects associated with the properties of water-soluble polymers are presented. The role of interfaces in catalysis by polymer structures is established and the possibilities of reaction rate increase upon concentrating the substrate in various catalyst areas are shown.

2
Amphiphilic Monomers and Polymers: Classification and Conformational Properties

Amphiphilicity is the key feature which influences the properties of water-soluble polymers in aqueous solutions. Hydrophilic compounds are well soluble in water, but hydrophobic ones are not. Amphiphilic compounds occupy an intermediate position, being able to level off the unprofitable interactions between water and hydrophobic compounds. This applies both to low and high molecular weight compounds. As already indicated, the earliest attempts to formulate the principles of organization in amphiphilic polymer systems led to the development of a simple HP model in which monomers of amphiphilic polymers were divided on a binary alphabet principle into the hydrophilic and hydrophobic [20, 21]. This model was promising from the viewpoint of considering the competition of hydrophobic interactions with the interactions of good solvent type between water molecules and hydrophilic monomer units. The principal disadvantage of the HP model is that it does not take into account the fact that the monomer units, which are considered as hydrophilic, consist actually of hydrophilic and hydrophobic parts, and are actually amphiphilic. This imposes certain restrictions on their behavior: for purely hydrophobic or hydrophilic monomer units, the location only in hydrophobic or hydrophilic media should be suggested; for amphiphilic ones, the location at interfaces is most probable.

In Refs. [24, 25], a two-dimensional thermodynamic classification of nonionic monomers was proposed, which took into account three possible preferential locations of a monomer unit (location either in the hydrophilic or the hydrophobic phase or at the interface between them). The proposed classification incorporates gradations by affinity to polar and nonpolar phases and by interfacial activity (Fig. 3).

Each monomer is ascribed with a two-dimensional coordinate, of which the abscissa dimension corresponds to the affinity to the polar (water) or the nonpolar phase (hexane) and the ordinate dimension corresponds to interfacial activity. The standard free energy of partition between water and hexane is used as a quantitative parameter for the abscissa axis (ΔF_{part}), whereas the standard energy of adsorption at the interface is used for the ordinate axis (ΔF_{ads}). Both parameters are normalized by the kT factor. The normalized values are denoted as Δf_{part} and Δf_{ads}, respectively. Thus,

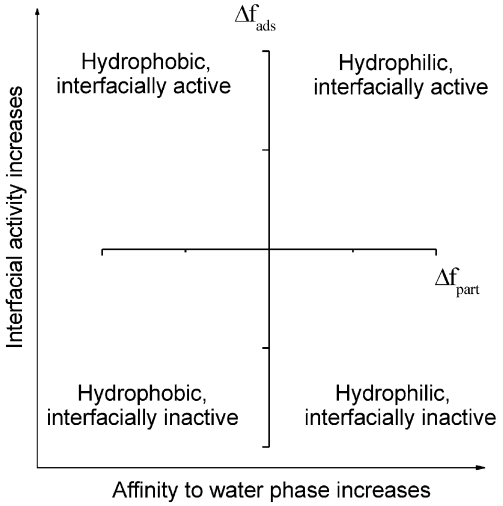

Fig. 3 Two-dimensional diagram of phase affinity and interfacial activity, general view. (Adapted from Ref. [25])

a four-quadrant diagram is constructed. Each quadrant involves a special class of monomers: hydrophobic interfacially active, hydrophobic interfacially inactive, hydrophilic interfacially inactive and hydrophilic interfacially active substances. Each of the two parameters used in the diagram appears as a quantitative tool for "one-dimensional" classification for a series of compounds. Indeed, a scale of *n*-octanol–water partition coefficients [26] and reverse-phase chromatographic retention parameters [27] are widely used to characterize the hydrophobicity of compounds; the concept of hydrophilic–lipophilic balance [28] was introduced for classification of surfactants according to their emulsifying properties. In the two-dimensional classification, both the potential for localization at the interface and the affinity to bulk phases are taken into account for several monomers, which allowed them to be classified on a broader basis.

The standard free energy of partition was calculated from water–hexane partition coefficients:

$$\Delta f_{\text{part}} = \ln P = \ln \frac{c_{\text{w}}^0 - c_{\text{h}}}{c_{\text{h}}}, \tag{1}$$

where P is the partition coefficient, c_{h} is the concentration in hexane, and c_{w} is the concentration in water.

The standard free energy of adsorption from either bulk phase was calculated from interfacial tension isotherms:

$$\Delta f_{\text{ads}}^{\text{b}} = \ln \left[1 + \frac{1}{RT\tau} \left(\frac{\gamma^0 - \gamma}{c_{\text{b}}} \bigg|_{c_{\text{b}} \to 0} \right) \right], \tag{2}$$

where Δf^{h}_{ads} is the standard free energy of adsorption from a bulk phase, c_b is the concentration in the bulk phase, τ is the thickness of the surface layer, and $\gamma^0 - \gamma$ is the interfacial pressure at the water–hexane interface.

When two contacting liquid phases are in equilibrium, the adsorption of surfactant at the interface can take place from either of them. Accordingly, standard Gibbs energies of adsorption can be calculated for each phase using Eq. 2.

Several monomers of water-soluble polymers were analyzed with the help of the proposed two-dimensional diagram (Figs. 4 and 5, Scheme 1). In Fig. 4, the data for four synthetic monomers, *N*-vinylcaprolactam (VCL), *N*-vinylpyrrolidone (VP), *N*-isopropylacrylamide (NIPA), and 1-vinylimidazole (Vim), at different temperatures are presented, and in Fig. 5, the data for eight amino acids are shown.

Three of the four synthetic monomers (NIPA, Vim, and VP) fall into the quadrant for hydrophilic interfacially active compounds; VCL finds itself in that for hydrophobic interfacially active ones and has the highest interfacial activity among the four. All the synthetic monomers considered become more hydrophobic upon temperature increase, as indicated by the decrease of Δf_{part}. VCL and VP become more interfacially active (Δf_{ads} increases) at elevated temperatures, while Vim shows the reverse behavior. Δf_{ads} of NIPA is almost insensitive to the temperature regime. For all the monomers, $|\Delta f_{part}| < |\Delta f_{ads}|$ (except NIPA at 10.5 °C) and it may be stated that higher affinity to the interface than to bulk phases is the key factor for those compounds.

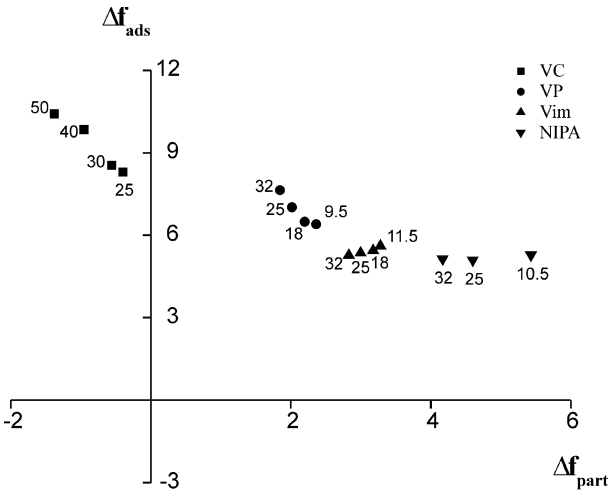

Fig. 4 Two-dimensional diagram for monomers of amphiphilic water-soluble polymers. The *numbers next to the points* are the measurement temperatures in degrees Celsius. (Adapted from Ref. [25])

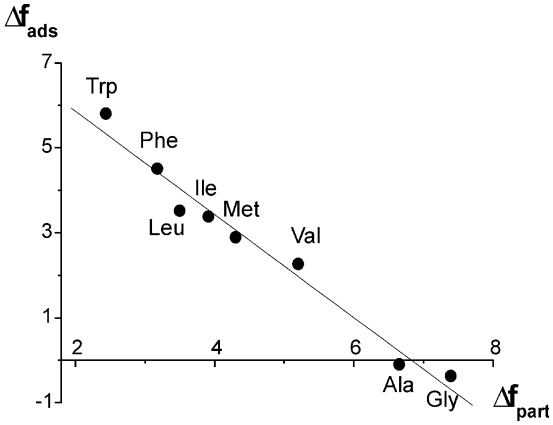

Fig. 5 Two-dimensional classification diagram for natural amino acids at 25 °C. (Adapted from Ref. [24])

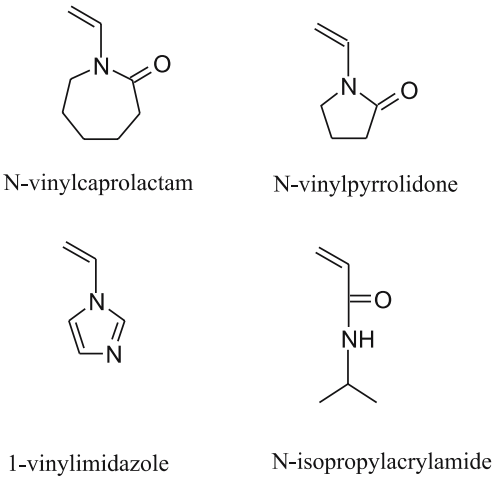

Scheme 2 Monomers characterized with the help of the two-dimensional diagram

The main feature of the amino acid diagram is that Δf_{ads} shows satisfactory linear correlation with Δf_{part}, with a slope of 1.22. Interfacial activity becomes stronger as the hydrophobicity of the amino acid residues increases. Since the amino acids have very hydrophilic amino and carboxyl groups, it may be said that the hydrophobicity increase enhances the amphiphilic character of the amino acids.

Thus, it was shown that many building blocks of natural and synthetic polymers are amphiphilic and interfacially active. For the monomers of several important water-soluble polymers, interfacial activity prevails over affinity to either bulk phase. Accordingly, it appears relevant to try to predict

which properties the polymers consisting of interfacially active amphiphilic monomer units may possess.

Vasilevskaya et al. [22, 23] proposed an extended model of the monomer unit in which the amphiphilic character of the latter was taken into account (HA model). Figure 2b illustrates the simplest dumbbell model of an amphiphilic monomer unit constructed from hydrophilic and hydrophobic segments. Within this model, hydrophobic segments represent nodes of a backbone, while polar segments are side groups attached to the nodes. It was shown that in such a model, conformational properties of amphiphilic polymers, especially in the globular state, may differ materially from those predicted by the HP model. In particular, it turned out that the globules formed by macromolecules containing amphiphilic monomer units are not spherical (Fig. 6). It was found that the amphiphilicity and interfacial activity of monomer units are the main reasons for the unusual conformational properties of the corresponding polymers.

The property of the polymers in question to form nonspherical nanostructures was confirmed in experimental studies. Shih et al. [29] synthesized alternating copolymers of 1-alkenes with maleic anhydride. The maleic anhydride units were hydrolyzed to maleic acid units. Fully hydrolyzed macromolecules associated into microstructures of cylindrical and ellipselike shape. The cylindrical shape was characteristic of copolymers with octadecene and hexadecene moieties, while the copolymers with lower alkene copolymers (tetradecene, dodecene, decene, octene) formed ellipsoidal structures. Wataoka et al. [30] investigated the formation of nonspherical helices in a system of maltopentaose-carrying polystyrene (PS). The polymer was synthesized via the homopolymerization of vinylbenzyl maltopentaose amide (Scheme 3).

Its structure was characterized by small-angle X-ray scattering (SAXS) (Fig. 7a). In Fig. 7a, three SAXS profiles are presented. Two of them are calculated theoretically (lines 1, 2) and the third profile (open circles) represents experimental results. Both lines 1 and 2 are obtained using the model of a kinked cylindrical helix as imaged in Fig. 7b. For line 2, the partial aggregation of the helices is taken into account. The theoretical and experimental

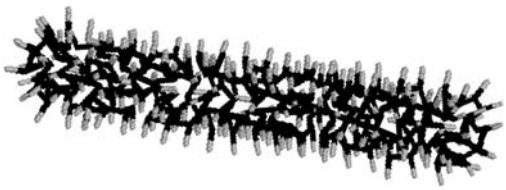

Fig. 6 Typical cylinder-shaped globules of polymers containing amphiphilic monomer units. *Darker spots* denote hydrophobic backbone nodes inside the core, *lighter spots* are hydrophilic side groups comprising the shell of the globule. (Adapted from Ref. [24])

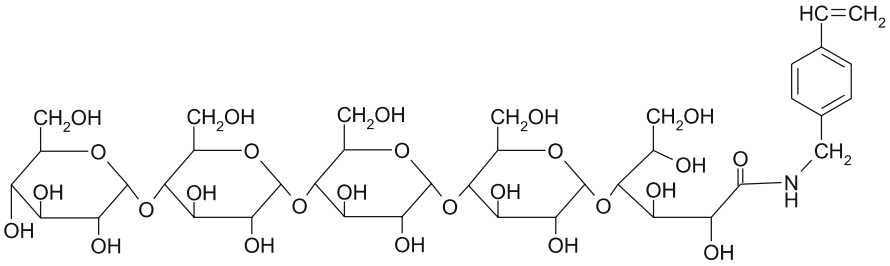

Scheme 3 Maltopentaose-carrying styrene macromonomer

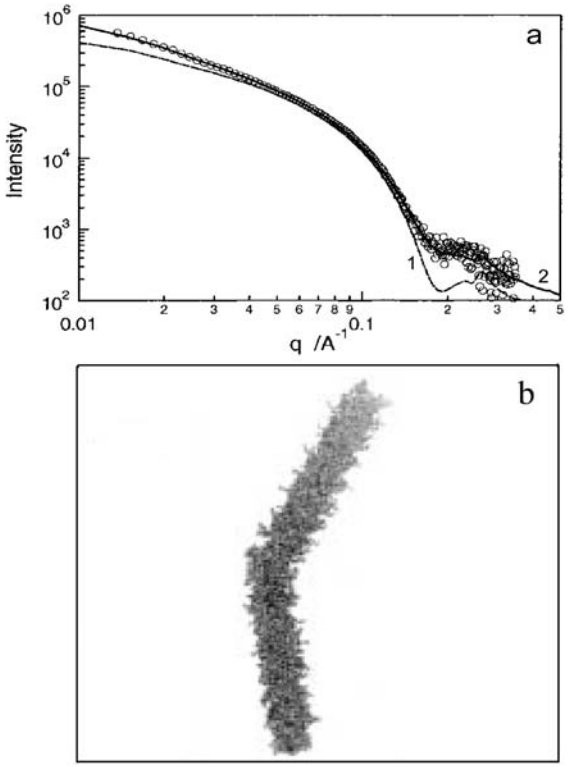

Fig. 7 **a** Scattering profiles for maltopentaose-carrying polystyrene. *Line 1* represents the calculated profile directly from the molecular model (see **b**) and *line 2* is calculated taking into account the effect of aggregation and backbone-folding. *Open circles* show the observed small-angle X-ray scattering profile of the copolymer in solution. **b** Molecular model of maltopentaose-carrying polystyrene. (Adapted from Ref. [30])

SAXS profiles shown in Fig. 7a coincide at most scattering vector values, which suggests that the proposed model satisfactorily describes the nanostructures formed in solution of maltopentaose-carrying PS as having cylindrical shape.

Theoretical line 2 fits best the experimental results, indicating that the observed cylindrical helices are prone to slight aggregation in water solutions.

The recent study of Thünemann et al. [31] showed the possibility of formation of cylindrical and disk-shaped nanostructures in aqueous solutions of polyampholytic copolymers of styrylmethyl(trimethyl)ammonium chloride (SMTMAC), methacrylic acid (MAA), and methyl methacrylate (MMA) complexed with perfluorododecanoic acid (PFDA) (Scheme 4). Cationic PFDA interacted with anionic SMTMAC to give neutral moieties, which were prone to association, while negatively charged groups of MAA stabilized the macromolecules from macroscopic phase separation. As a result, anisotropic nanostructures were obtained, the formation of which was confirmed by SAXS (Fig. 8). In Fig. 8, experimentally obtained pair distribution functions of the typical structures are plotted along with the theoretical distribution functions for an idealized cylinder with a diameter of 3.0 nm (Fig. 8a) and for a disk with a height of 2.2 nm (Fig. 8b). The intersection points with the abscissa of the distribution functions correspond to the characteristic dimensions of the idealized cylinder or disk. Good consistency was observed between the theoretical and experimental distribution functions, which allowed a conclusion to be made about the formation of nonspherical structures of cylindrical and disklike shape in the systems of amphiphilic copolymers of SMTMAC, MAA, and MMA complexed with PFDA.

Some attention should be also paid to the fact that some copolymers with special sequence distribution do not assume cylindrical shape within the HA model. For example, this is the case for protein-like sequences. Protein-like sequences correspond to a copolymer which forms globules with a hydrophobic core and a hydrophilic shell showing no tendency to aggregation. Protein-like copolymers have been previously studied within the HP model [32–34]. Application of the more realistic HA model showed that the globules formed by protein-like copolymers under worsening solvent quality assume conventional spherical shape and show no tendency to aggregate [23]. The stability for HA model protein-like copolymers is much higher than for those within the HP model.

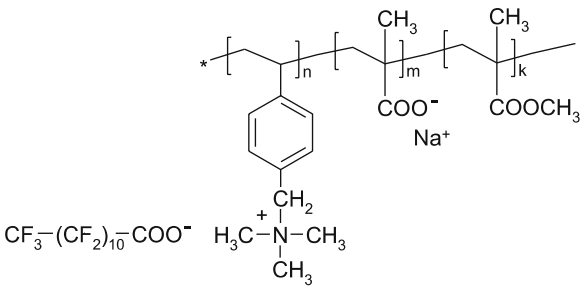

Scheme 4 Polyampholyte complexes with perfluorodecanoate anion

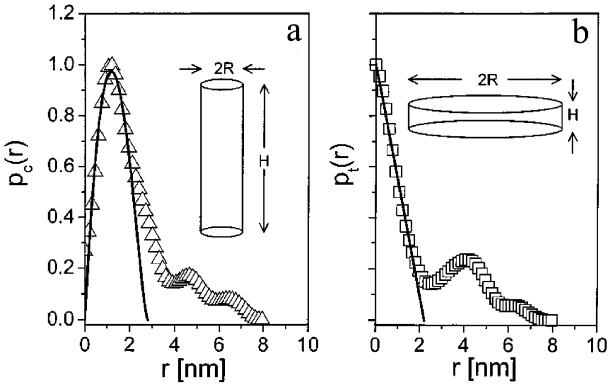

Fig. 8 Pair distribution functions of complexes of **a** cylindrical symmetry (57% styrylmethyl(trimethyl)ammonium, 16% methacrylic acid, 27% methyl methacrylate) and **b** disklike symmetry (79% styrylmethyl(trimethyl)ammonium, 13% methacrylic acid, 8% methyl methacrylate). The curves which were calculated from the scattering data are represented by *triangles* and *squares*. *Solid lines* represent the distribution functions of **a** an idealized cylinder with a diameter of 3.0 nm and of **b** a disk with a height of 2.2 nm. The *insets* depict idealized symmetries of the particles. (Adapted from Ref. [31])

3
Nanostructure Formation in Solutions of Thermosensitive Polymers

The properties associated with the amphiphilic monomer units are strongly exemplified in thermosensitive water-soluble polymers, typical examples of which are shown in Scheme 5. Thermosensitive polymers possess a lower critical solution temperature (LCST) in water solutions. Due to their sharp response to temperature variation, they are widely used in various scientific and technological applications. Drug and gene delivery [1–3], chromatographic [9, 10], membrane technology [11, 12], and catalyst immobiliza-

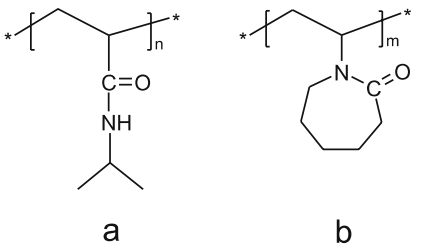

Scheme 5 Typical thermosensitive polymers: **a** poly(*N*-isopropylacrylamide), **b** poly(*N*-vinylcaprolactam)

tion [35] applications have been reported. The property of thermosensitivity is closely connected with the amphiphilicity of monomer units. At low temperature, water is a good solvent for chains of thermosensitive polymers owing to the formation of hydrogen bonds between water molecules and hydrophilic moieties of the macromolecules. Monomer units of the latter also contain hydrophobic CH_2 groups, which are involved in unprofitable hydrophobic interactions. It is well known that temperature increase leads to the intensification of hydrophobic interactions in water [36]. While at low temperature the interactions between water and hydrophilic groups are stronger than the hydrophobic interactions, at higher temperature the latter prevail, which leads to the coil-to-globule transition of macromolecular chains and further aggregation. The coil-to-globule transition may be directly observed in solutions of thermosensitive polymers, both on addition of surfactants [37–40] and in surfactant-free solutions [41–43]. The transition was confirmed by dynamic and static light scattering methods. The collapse of polymer chains was identified by a sharp decrease in the radius of gyration and the hydrodynamic radius of the macromolecules. The formation of globules in surfactant-free solutions of poly(VCL) (PVCL) [41] and poly(NIPA) (PNIPA) [42, 43] can be detected only at extremely low concentrations (below 10^{-3} g/L). At higher concentrations, the collapse of the polymer chains is accompanied by aggregation. However, upon addition of small amounts of surfactants, the aggregation may be suppressed, whereas the intramolecular aggregation is still possible. The corresponding studies were conducted both for PVCL [37, 38] and PNIPA [39, 40] in solutions with relatively high polymer content (approximately 1 g/L). As in the surfactant-free studies, a decrease in hydrodynamic radius was observed upon temperature increase (Figs. 9, 10), which indicated the formation of the globular structures stabilized against aggregation by a surfactant shell.

Globules represent the simplest structures of thermosensitive polymers of the nanometer scale. In the last few years, a series of works were aimed at obtaining nanoscale objects with a complex structure based on PVCL and PNIPA. The amphiphilic character of PVCL and PNIPA chains allowed them to be conjugated both with hydrophilic and with hydrophobic species to yield ordered self-associating systems in solution and at the interface. The main approach for the design of such systems is based on synthesis of block copolymers, which organize in core–shell structures in solution. In particular, block and/or graft copolymers of NIPA and ethylene oxide (PNIPA-*b*-PEO and PNIPA-*g*-PEO) [44–47], NIPA and propylene oxide [48], NIPA and styrene (PNIPA-*b*-PS) [49, 50], NIPA and lactic acid [51], VCL and EO (PVCL-*b*-PEO) [52, 53] were synthesized. Qiu and Wu [44] obtained PNIPA-*g*-PEO by radical copolymerization of PNIPA and PEO macromonomers capped with a methacrylate monomer unit. The copolymers underwent a transition accompanied by the formation of a nanostructure with a hydrophobic PNIPA core and a hydrophilic PEO shell. The character of aggregation was

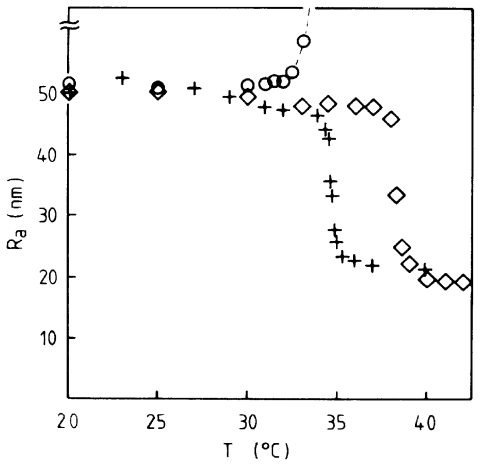

Fig. 9 Temperature dependencies of poly(*N*-isopropylacrylamide) (*PNIPA*) hydrodynamic radius as a function of surfactant concentration: *circles* 0, *crosses* 1.1, *squares* 1.8 mmol/L. (Adapted from Ref. [39])

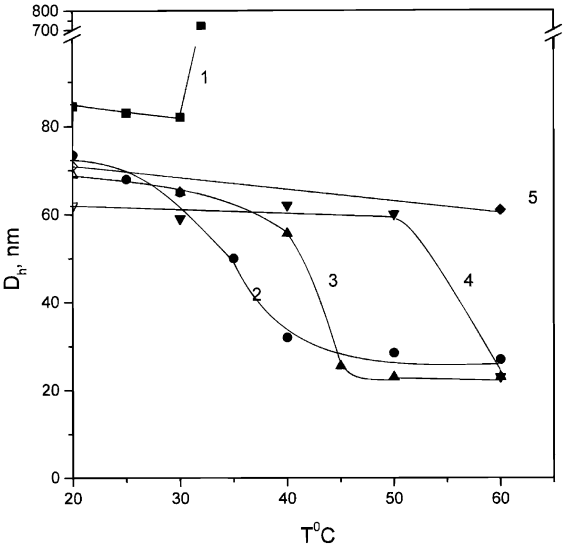

Fig. 10 Temperature dependencies of poly(*N*-vinylcaprolactam) (PVCL) hydrodynamic diameter as a function of surfactant concentration: *1* 0, *2* 0.25, *3* 0.5, *4* 1, *5* 3 mmol/L sodium dodecyl sulfate. (Reprinted with permission from Ref. [37]. Copyright 1998 American Chemical Society)

molecular-weight-dependent: for shorter chains, intermacromolecular aggregation dominated, as indicated by an increase in R_h at the temperature of the collapse (Fig. 11a), while for longer chains, the coil-to-globule transition of

individual macromolecules was observed, as shown by a drop in R_h of polymer particles (Fig. 11b). It should be noted that in the case of longer chains, the intrachain collapse is observed at relatively high concentrations (approximately 0.1 g/L), in contrast to the individual PNIPA chains, for which very low concentrations are needed to detect the coil-to-globule transition.

Diblock copolymers of NIPA and EO showed somewhat different behavior [45]. The copolymers were synthesized using NIPA monomer and PEO-containing macroinitiator. The copolymers aggregated at high temperature with no collapse of individual macromolecules. The essential feature of the polymers in question consisted in the strong sensitivity of the shape of the particles to the polymer concentration and to the molar ratio of EO to NIPA monomer units. At low polymer concentration, the shape of the aggregates was mainly spherical, as indicated by the low R_g/R_h values (Fig. 12). The R_g/R_h ratio is informative of the shape of particles in solution. Anisotropic particles, such as rods and coils, possess high values of the ratio, while for particles of spheroid form, low values of the ratio are observed (for spher-

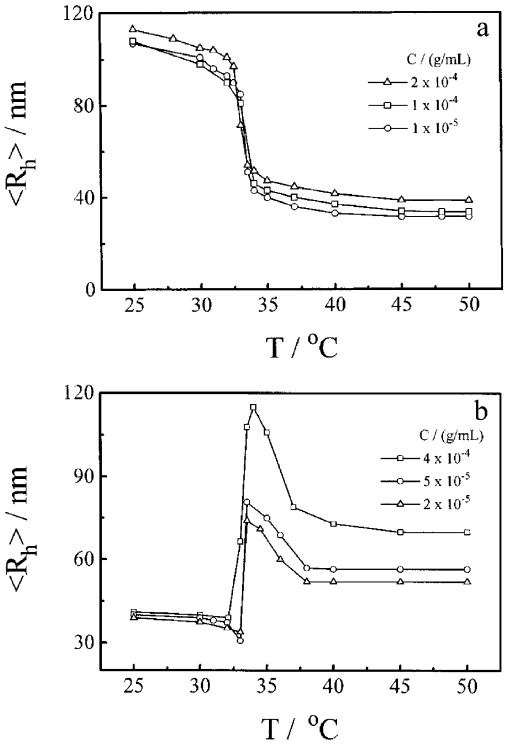

Fig. 11 Temperature dependencies of the hydrodynamic radius of PNIPA-*g*-PEO **a** high molecular weight and **b** low molecular weight chains in water at different polymer concentrations. *PEO* poly(ethylene oxide). (Adapted from Ref. [44])

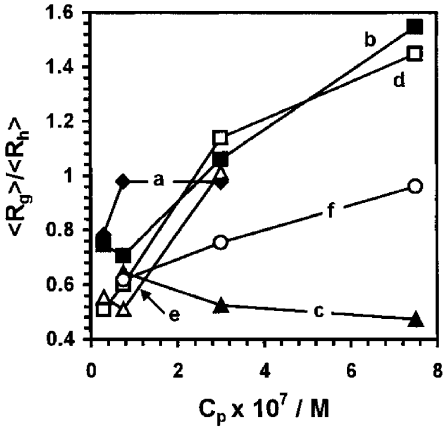

Fig. 12 Ratio of the average radius of gyration to the average hydrodynamic radius of the aggregates as a function of copolymer concentration. Ratios of NIPA-to-EO monomer units: *a* 151, *b* 69, *c* 13, *d* 244, *e* 107, *f* 27. *NIPA N*-isopropylacrylamide, *EO* ethylene oxide. (Reprinted with permission from Ref. [45]. Copyright 2002 American Chemical Society)

ical globules, $R_g/R_h = 0.78$; for rods, $R_g/R_h > 2$; for coils in a θ solvent, $R_g/R_h = 1.78$). Spherical PNIPA-*b*-PEO nanoparticles with high EO content showed in some cases anomalous behavior (Fig. 12, lines c and f): R_g/R_h was lower than the theoretical value, which was explained by the fact that the cores of those particles were much denser than their surface. Upon increase of concentration, the R_g/R_h value of most of the copolymers increased, which indicated that the aggregates assumed anisotropic shape: for the PNIPA-*b*-PEO nanostructures, an ellipsoidal form was suggested (Fig. 12, lines a, b, d, and e).

Besides block copolymers of NIPA and EO, analogous systems based on VCL were reported [52]. PVCL-*g*-PEO was synthesized by copolymerization of VCL and PEO macromonomer end-capped with a methacrylate moiety. The graft copolymers showed unusual conformational behavior depending on temperature (Fig. 13). At temperatures slightly above the LCST, the formation of huge polymer aggregates of 2-μm size was observed. On further heating, the thermosensitive core of the aggregates decorated with PEO grafts shrank readily to give clusters of 300–400 nm in diameter. Increasing the degree of grafting led to larger aggregates at 60 °C owing to a looser PVCL core at a high grafting degree. PVCL-*g*-PEO copolymers were shown to be a prospective material for drug delivery as they were characterized by low cytotoxicity [53].

A new way of obtaining nanostructures in systems of thermosensitive polymers by combining them with hydrophilic species was proposed by Bronstein et al. [54]. The core–shell nanoparticles were obtained by stabilization of the globular conformation of PVCL in aqueous solutions at 45 °C on add-

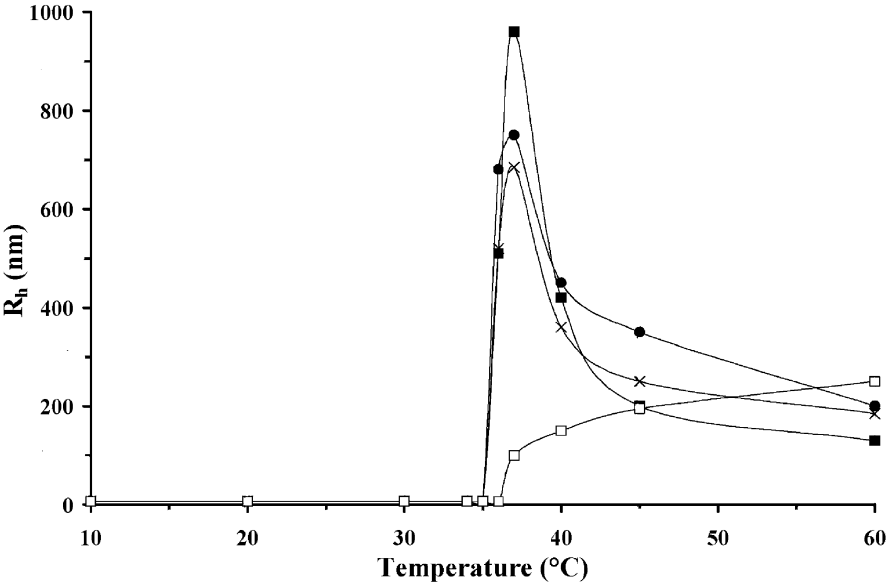

Fig. 13 Temperature dependencies of the hydrodynamic radius of PVCL-*g*-PEO for copolymers with different degrees of grafting: *squares* 20 wt % PEO, *crosses* 35 wt % PEO, *circles* 50 wt % PEO, at a copolymer concentration of 0.65 mg/mL; *open squares* 20 wt % at a copolymer concentration of 0.065 mg/mL. (Adapted from Ref. [52])

ition of $CoCl_2$. As visualized by transmission electron microscopy (TEM), on cooling PVCL solutions treated with $CoCl_2$ to room temperature, the nanoparticles of 11-nm size were present in the system (Fig. 14a, b). Addition of $CoCl_2$ at room temperature resulted in large aggregates of 200 nm in diameter, as shown in Fig. 14a, inset. A ^{13}C NMR study demonstrated that the spectra of PVCL solutions treated with $CoCl_2$ are identical to those of untreated ones, meaning that VCL units retain their mobility after interaction with Co^{2+} ions. Thus, they do not stay in a compact conformation characteristic of a collapsed state after cooling. To clarify the exact conformation of the particles obtained, the TEM grid was stained with OsO_4, which allowed visualization of the parts of the PVCL macromolecules not coordinated to Co^{2+} ions (Fig. 14c). Staining resulted in loose spherical structures with dark cores. It was suggested that the core consisted of certain areas of PVCL chains cross-linked by multivalent Co ions, while the rest of the molecules protruded through the cross-linked area forming the outer layer visualized in the stained image by loose coronas (Fig. 15).

Some works were reported in which thermosensitive polymers were conjugated with hydrophobic groups. End-capping random poly(NIPA-*co*-dimethylacrylamide) [55] and grafting poly(NIPA-*co*-hydroxymethylacrylamide) [56] with cholesterol moieties led to self-associating polymers with different morphologies. By dissolution of the copolymers in dimethylfor-

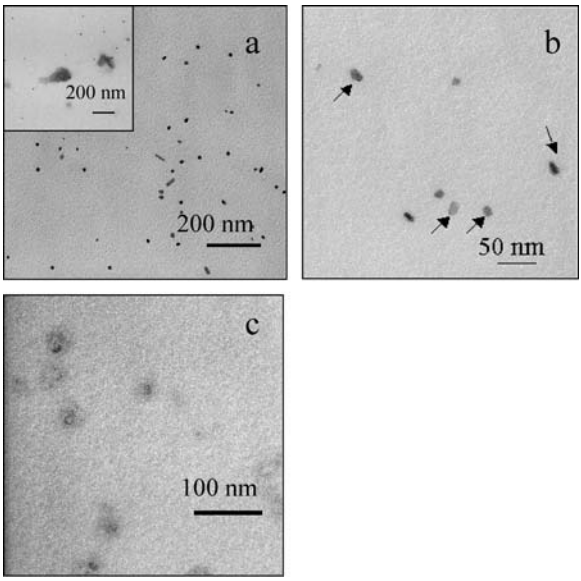

Fig. 14 Transmission electron microscopy (*TEM*) images of PVCL-Co nanoparticles. **a** Nanoparticles obtained upon cooling PVCL solutions treated with $CoCl_2$ at 35 °C (above the lower critical solution temperature). The *inset* shows large aggregates formed upon adding $CoCl_2$ at room temperature. **b** Enlarged image of PVCL nanoparticles. **c** PVCL-Co nanoparticles stained with OsO_4. (Reprinted with permission from Ref. [54]. Copyright 2005 American Chemical Society)

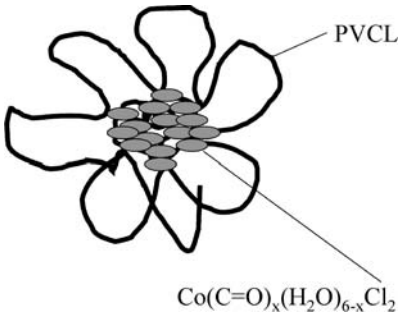

Fig. 15 A core–shell model of PVCL-Co nanoparticles. (Adapted from Ref. [54])

mamide and further dialysis against water, it was possible to obtain copolymer micelles of 30-nm size below the LCST. Heating the dialyzed solutions over 40 °C led to aggregation of the micelles with formation of particles of 200-nm size. Freeze-drying the micellar solutions led to nanoparticles of cuboid, starlike, and spherical shapes depending on the concentration of the initial micellar solution when imaged with TEM (Fig. 16).

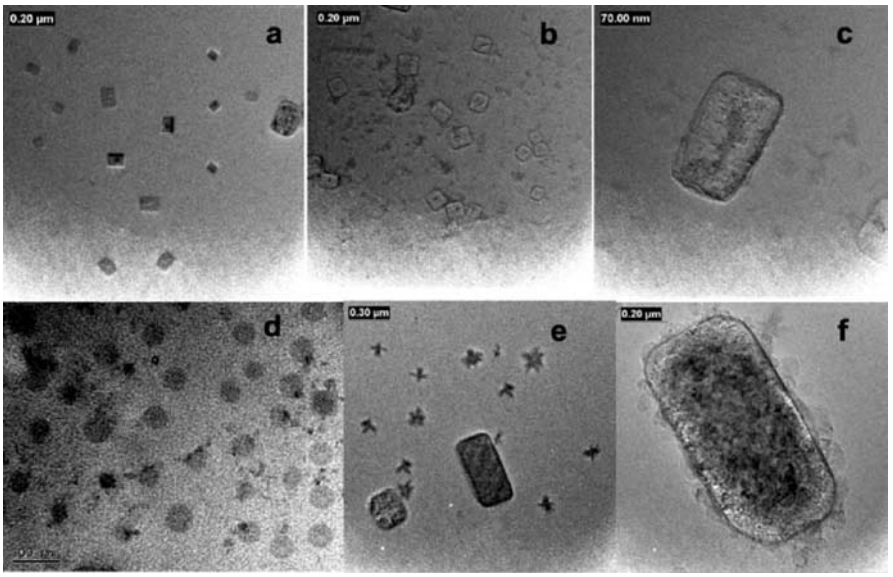

Fig. 16 TEM pictures showing nanoparticles of cholesteryl end-capped poly(NIPA-co-dimethylacrylamide). The nanoparticles were obtained by the dialyzing dimethylformamide solutions of copolymers against water and subsequent freeze-drying. The initial concentrations of the copolymer in dimethylformamide were **a**–**c** 0.35 wt %, **d** 0.1 wt %, **e**, **f** 1.2 wt %. **a**, **c**–**f** were obtained for the copolymer with $M_w = 3400$; **b** was obtained for the copolymer with $M_w = 8000$. (Reprinted with permission from Ref. [55]. Copyright 2003 Elsevier)

Diblock PNIPA-*b*-PS was synthesized by the reversible addition–fragmentation chain transfer method using PS macroinitiators [49]. The behavior of the copolymers was dependent on the length of the NIPA blocks. Shorter NIPA blocks formed micelles 120 nm in diameter, while the copolymer with longer NIPA blocks associated in huge nonstructured aggregates of 1.2 μm. Upon heating, the aggregates shrank, whereas the size of the micelles did not change considerably. Microcalorimetric studies have shown that the phase transition of the copolymer with longer PNIPA blocks takes place at the same temperature as that of PNIPA homopolymer, meaning that separate PNIPA chains are responsible for shrinking of the aggregates. The collapse of PNIPA-*b*-PS with shorter PNIPA blocks is characterized by lower temperatures of the transition and broad calorimetric peaks, which are characteristic of random PNIPA-PS copolymers (4% of styrene [50]). Indeed, such copolymers are likely to consist of short NIPA blocks separated by styrene monomer units. Thus, the character of the microcalorimetric peaks might be determined by the length of the PNIPA blocks.

As a conclusion to this part, one may state that thermosensitive polymers represent prospective macromolecules for the design of nanoparticles the

properties of which are temperature-dependent. Owing to the amphiphilicity of their chains, they can manifest both hydrophilic and hydrophobic properties depending on solvent quality. Therefore, when combined with hydrophobic or hydrophilic moieties, they can self-organize in nanostructures under appropriate conditions.

4 Catalytic Properties of Polymer Associates in Aqueous Media

Catalytic properties of water-soluble synthetic polymers have long been a subject of considerable interest, which was inspired by the investigation of enzyme action mechanisms. As was shown in the works of Overberger et al. [57, 58], Kunitake et al. [59, 60], and Kirsh et al. [61, 62], hydrophobically and electrostatically driven adsorption of substrates at the chains of polymer catalysts is one of the major factors that define the catalytic activity being analogous to the forces that play a leading role in enzyme–substrate interactions. It is worth mentioning here that enzymatic mechanisms of catalysis were also realized in imprinted polymers. Those studies showed that arranging active groups of the catalyst in a stiff spatial configuration with the help of removable template molecules can lead to analogues of enzyme binding sites having a geometrical match with the substrate. Several reviews have already been published on this issue [16, 17], so imprinted polymers will not be considered in this article.

Substrate–catalyst interaction is also essential for micellar catalysis, the principles of which have long been established and consistently described in detail [63–66]. The main feature of micellar catalysis is the ability of reacting species to concentrate inside micelles, which leads to a considerable acceleration of the reaction. The same principle may apply for polymer systems. An interesting way to concentrate the substrate inside polymer catalysts is the use of cross-linked amphiphilic polymer latexes [67–69]. Liu et al. [67] synthesized a histidine-containing resin which was active in hydrolysis of *p*-nitrophenyl acetate (NPA). The kinetics curve of NPA decomposition in the presence of the resin was of Michaelis–Menten type, indicating that the catalytic act was accompanied by sorption of the substrate. However, no discussion of the possible sorption mechanisms (i.e., sorption by the interfaces or by the core of the resin beads) was presented.

The latexes prepared in the group of Ford [68, 69] consisted of hydrophobic monomers and a cross-linker, i.e., styrene, methacrylate monomers with various substitutes in the ester moiety, divinylbenzene, and hydrophilic monomers bearing charged groups, viz., styrylmethyl(trimethyl)ammonium and styrylmethyl(tributyl)ammonium cations. The latexes were catalytically active in reactions of decarboxylation of 6-nitrobenzioxazole-3-carboxylate (Scheme 6) and *p*-nitrophenyl hexanoate hydrolysis (Scheme 7, $n = 6$).

The main reason behind the acceleration was suggested to be the concentrating of substrates in a small volume of the latex phase and an increase in intrinsic rate constants, obviously due to the change in environment from the polar medium (water) to the hydrophobic one (latex), since 6-nitrobenzioxazole-3-carboxylate is stabilized in water by hydrogen bonding, while in latex such stabilization does not take place. Hydrolysis of *p*-nitrophenyl hexanoate in the medium of the latexes was found to have a higher rate with respect to the hydrolysis by OH^- ions in water mainly owing to the concentrating effect of both substrate and catalyst (OH^- ions), as the variation of the intrinsic rate constant was minimal. Data on the catalytic properties of the latexes are summarized in Table 1. The general tendency observed consisted in the fact that the largest rate constants were characteristic for the latexes containing long hydrophobic aliphatic tails in methacrylate and tetraalkylammonium monomer units capable of interacting effectively with hydrophobic substrates.

Interfacial adsorption may also become an effective tool to increase significantly the rate of catalytic reaction since it leads to the concentrating of reactants at the boundaries of immiscible phases, so that the interfacial layer becomes a reactor of nanoscale thickness (*surface nanoreactor*). Recently, Vasilevskaya et al. [70] emphasized that the possibility to accelerate a catalytic reaction exists in surfactant-free miniemulsions, if both catalyst and substrate adsorb at the oil–water interfaces. At emulsion droplet interfaces, a significant concentrating effect may be achieved, since the concentration at interfaces may be several orders of magnitude higher than in bulk phases. Furthermore, the absence of surfactants guarantees that a considerable part of the interface is not occupied by foreign substances, providing greater possibilities for concentrating the reactants. It was shown that at a certain optimum size of miniemulsion droplets (normally around several hundred nanometers), a significant increase in reaction rate occurs compared with the case where the size of the droplets is

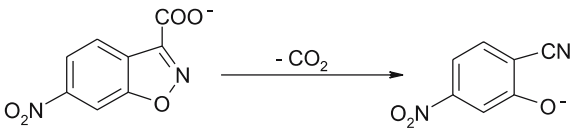

Scheme 6 Decarboxylation of 6-nitrobenzioxazole-3-carboxylate

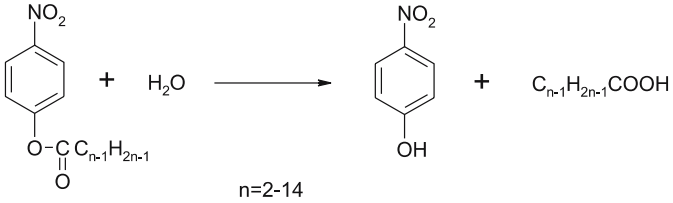

Scheme 7 Hydrolysis of *p*-nitrophenyl alkanoates

Table 1 Ratios of the rate constant in the presence of latex (k_{lat}) to that in water (k_w) for latexes of different composition. (Data from Ref. [69])

Latex type	Ester substitute in methacrylate monomer	k_{latex}/k_w	
SMTMA latexes	No methacrylate monomer	2.3	900
	n-Butyl	6.1	2900
	n-Hexyl	6.5	
	n-Octyl	9.5	4100
	n-Decyl	10.2	4400
	n-Dodecyl	10.7	
	Isobutyl	6.5	3300
	2-Ethylbutyl	6.1	
	2-Ethylhexyl	12.5	8300
	2-Chloroethyl	5.6	
	Butoxyethoxyethyl	5.8	400
	Ethoxyethoxyethyl	5.5	200
	Tetrahydrofurfuryl	7.1	3200
	Tetrahydropyranyl	5.6	
	Furfuryl	5.8	
SMTBA latexes	No methacrylate monomer	12.0	9600
	n-Butyl	15.7	6600
	2-Ethylhexyl	16.5	10 400

SMTMA styrylmethyl(trimethyl)ammonium, *SMTBA* styrylmethyl(tributyl)ammonium

either too small or too large, as well as with the case of complete phase separation. In Fig. 17, a series of dependencies of reaction rate vs. droplet radius are presented for different adsorption energy at the droplet interface, ε (in kT units). The positions of the maxima were found to be sensitive to ε: a lower energy of adsorption required a lower optimum size of the emulsion droplets. The reason for the presence of the reaction rate maxima in the dependencies is as follows: for small radii of the droplets the overall interfacial area is large, so a high interfacial concentration cannot be achieved, and if the droplets are too large, very few interfacial areas are available, thus reducing the probability that the catalyst and the substrate meet each other in those areas.

The analogous considerations are valid for polymer systems as well. Indeed, amphiphilic monomer units also tend to occupy interfacial areas of macromolecular associates as it is normal for low molecular weight surfactants to adsorb at polymer–poor solvent boundaries. And, if such interfacial groups of the polymer associate catalyze chemical transformation of a compound which tends to adsorb at the associate interfaces, this can result in unusual kinetics effects. Okhapkin et al. [18] studied the influence of temperature-induced aggregation on the catalytic activity of thermosensitive

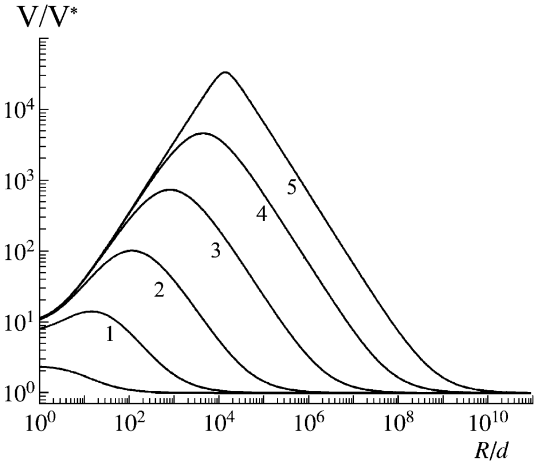

Fig. 17 Reaction rate in an emulsion as a function of emulsion droplet radius and adsorption energy of substrate and catalyst: 1 $\varepsilon = 2$, 2 $\varepsilon = 4$, 3 $\varepsilon = 8$, 4 $\varepsilon = 10$, 5 $\varepsilon = 12$, 6 $\varepsilon = 14$. The reaction rate in the emulsion is normalized by that in the homogeneous phase; the emulsion droplet radius is normalized by the diameter of a substrate molecule. (Adapted from Ref. [70])

copolymers of VCL and Vim (PVCL-Vim) and NIPA and Vim (PNIPA-Vim), which exist in a coiled state in aqueous or 2-propanol–water solutions at room temperature. The copolymers in both coil and aggregate states were tested as catalysts of NPA hydrolysis (Scheme 7, $n = 2$). As the aggregate state of such copolymers is reached by raising the temperature, the effects of aggregation and temperature on the catalytic properties of the copolymers overlapped. Therefore, the correlation of the catalytic properties with the aggregation was investigated using the reaction rate vs. temperature dependencies, which normally give a linear plot on semilogarithmic (Arrhenius) coordinates. The aggregation influenced the reaction rate along with temperature, producing a deviation from the linear law. Figure 18 shows the Arrhenius dependencies for the four copolymer catalysts, 1-methylimidazole and PVim as controls, at identical concentrations of imidazole groups. For 1-methylimidazole and PVim, the dependencies were quite linear, showing that those catalysts followed the Arrhenius-type behavior. For copolymer catalysts, the rate–temperature dependencies were not linear in Arrhenius coordinates. In the temperature range 35–45 °C, the growth law was faster than the linear one. When the temperature was raised further, the opposite effect was observed, viz., the reaction rate slowed down.

The relation between the catalytic and aggregation properties of the copolymers was shown using the dynamic light scattering method. Hydrodynamic radius distributions obtained by processing light scattering data showed that at temperatures below 35 °C the copolymers existed in the form

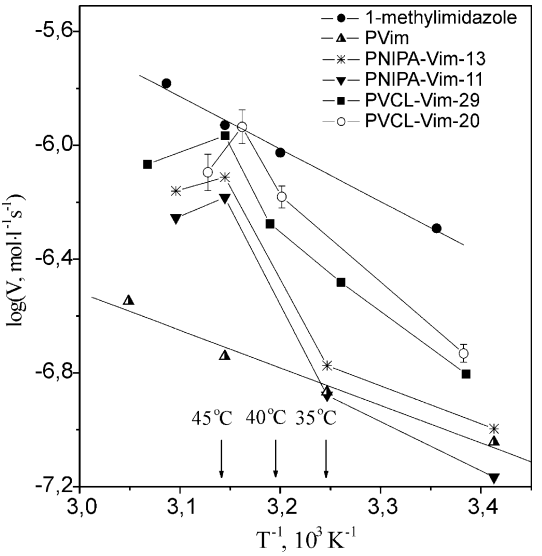

Fig. 18 Reaction rate of hydrolysis of *p*-nitrophenyl acetate as a function of inverse temperature. Thermosensitive imidazole-containing copolymers (PVCL-Vim, PNIPA-Vim), 1-methylimidazole and poly(1-vinylimidazole) act as catalysts. *Numbers in the copolymer abbreviations* denote the Vim content (in mole percent). *Vim* 1-vinylimidazole. (Adapted from Ref. [18])

of coils, while aggregates were formed upon heating above that temperature (Fig. 19). At low temperature the average radius of the polymer particles did not exceed 10 nm. Upon heating, new peaks at 100–200 nm emerged, indicative of the aggregation. For all the copolymers studied, the temperature intervals of aggregation preceded the temperature interval of rapid growth of the reaction rate in the region 35–45 °C. Thus, the observed acceleration of the reaction was found to be closely connected with the aggregation phenomenon in solutions of the thermosensitive copolymers.

A Michaelis–Menten profile of the catalyzed reaction was observed for the thermosensitive copolymers studied. In enzymatic catalysis, the catalytic act is preceded by the complex formation between catalyst and substrate. Because of the complex formation, enzymatic reactions follow Michaelis–Menten-type kinetics:

$$V = \frac{V_0 [S]}{K_m + [S]}, \tag{3}$$

where $V_0 = k_{cat}[E_0]$, k_{cat} is the first-order rate constant for breakdown of the substrate–catalyst complex, $[E_0]$ is the concentration of catalyst, $[S]$ is the concentration of substrate, and K_m is the Michaelis constant, which is the dissociation constant of the enzyme–substrate complex. For a PNIPA-Vim copolymer containing 11% of imidazole groups, a kinetics curve in

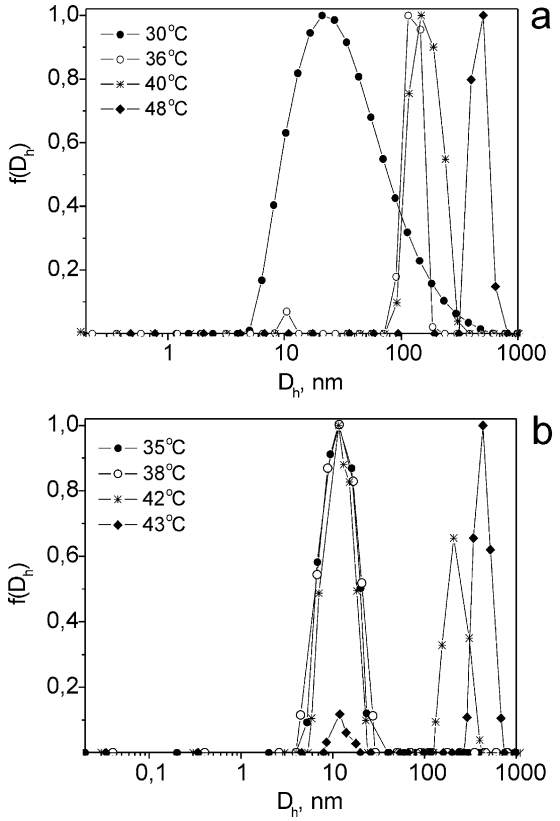

Fig. 19 Distribution functions of the hydrodynamic diameter for the imidazole-containing thermosensitive copolymers in 2-propanol–water solutions at various temperatures: **a** PNIPA-Vim, 11% of imidazole; **b** PVCL-Vim, 29% of imidazole. (Adapted from Ref. [18])

V–[S] coordinates was obtained which could be well fitted with Eq. 3 giving $V_0 = 8.6 \times 10^{-7}$ mol/L s and $K_m = 0.0105$ mol/L. It was possible to explain the phenomenon of enhanced catalytic activity of the copolymer aggregates in the following terms by taking that fact into account.

As PVCL-Vim and PNIPA-Vim form aggregates of submicrometer sizes at elevated temperature, NPA can adsorb at their interfaces forming a kind of "complex" with the outer polymer groups (Fig. 20). Both Vim and NPA are amphiphilic and their affinity to interface is high: when partitioned between hexane and water, their free energies of adsorption to the interface (from water) are 5.8 kT (14 kJ/mol) and 9.7 kT (24 kJ/mol), respectively, whereas the free energies of partition are 3.0 and –2.0 kT. Thus, the location at the phase boundaries is preferential for them, and can stimulate NPA and monomer units of Vim to concentrate at the interfacial areas of the polymer aggregates, which leads to the rapid progress of the reaction in those areas.

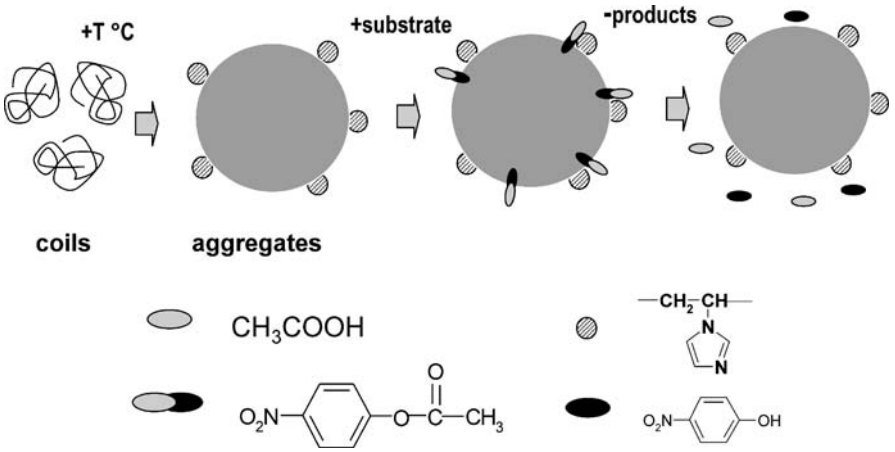

Fig. 20 Interfacial layer of PVCL-Vim and PNIPA-Vim aggregates as a catalytic nanoreactor. (Adapted from Ref. [18])

Furthermore, there can be some additional factors that increase the reaction rate at aggregate interfaces. First, both catalyst and substrate are specifically oriented in the interfacial layer owing to the polymer concentration gradient. This factor can lead to a specific mutual orientation of the interacting species, which is beneficial for an elementary act of the catalytic reaction. Second, the substrate molecules are subjected to a high stress owing to the polymer concentration gradient. The second factor should reduce the activation energy of the reaction as the stress increases the ground-state energy of the substrate molecules.

Binding to the interfaces of polymer aggregates may also result in specific catalytic effects in the case of homologous series of substrates. Lawin et al. [71] studied hydrolysis of *p*-nitrophenyl alkanoates (NPAlk) (Scheme 7) in the presence of hydroxide ions which was mediated by polymer micelles of poly(*N*-(*n*-dodecyl)-4-vinylpyridinium-*co*-*N*-ethyl-4-vinylpyridinium) bromide (PDEVP). PDEVP was reported to form compact micelles with a definite surface, which is mainly covered by charged pyridinium moieties but having as well some hydrophobic areas in the structure. The micelles were supposed to bind the substrates by hydrophobic surface areas and hydroxide ions by positively charged pyridinium ions. The diverse character of the concentration dependencies of the reaction rate was observed for substrates with different chain length (Fig. 21). This was associated with the possibility of aggregation of NPAlk in aqueous solutions suggested in a work of Guthrie [72]. In Fig. 21, one may observe a kind of kink at the concentration dependencies of $n = 8$ and $n = 10$. The kinks of the curves were identified with the critical aggregation concentrations (CACs) of the substrates, meaning that at higher NPAlk concentrations PDEVP associates rather with NPAlk aggregates than

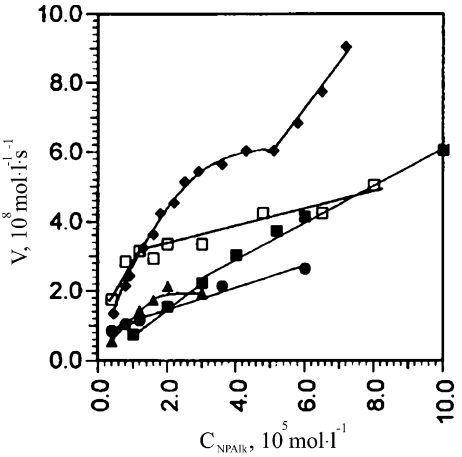

Fig. 21 Reaction rate versus substrate concentration for hydrolysis of *p*-nitrophenyl alkanoates (*NPAlk*) in the presence of poly(*N*-(*n*-dodecyl)-4-vinylpyridinium-*co*-*N*-ethyl-4-vinylpyridinium) bromide (*PDEVP*): *closed squares* $n = 6$, *diamonds* $n = 8$, *open squares* $n = 10$, *circles* $n = 12$, *triangles* $n = 14$. (Adapted from Ref. [71])

with individual molecules (Fig. 22). In particular, the CAC of $n = 8$ is rather high, which ensures the possibility of saturation of the PDEVP surface with individual molecules of the substrates. At the CAC, the newly formed aggregates start to associate with the PDEVP surface contributing to an additional increase of the reaction rate. In the case of $n = 10$, the CAC is rather low, so the saturation by individual molecules is not attained before the kink. For $n = 6$, the kink is not observed at the concentrations studied, obviously because the substrate has a relatively short hydrophobic tail and its critical aggregation concentration is too high to be observed in the concentration range studied. Thus, it was shown that the adsorption of the substrate to the polymeric catalyst may lead to complex catalytic effects which depend on the phase behavior of both substrate and catalyst.

Wang et al. [73–76] performed a study of the catalytic activity of a silicon-based polymer obtained by polycondensation of 4-bis[(3-dimethyl-ethoxy-

Fig. 22 Representation of different types of association between PDEVP and NPAlk: **a** adsorption of individual molecules of the substrate, **b** adsorption of aggregates of the substrate. (Adapted from Ref. [71])

silyl)propyl]aminopyridine (Scheme 8). The influence of buffer composition [73, 76], salt content [73], surfactant [74], and polymer concentration [75, 76] was investigated. It was shown that polymer **1** (Scheme 8) revealed specificity to NPAlk of certain length; moreover, the specificity was very sensitive to the solvent composition. The reaction carried out in buffered aqueous solutions was substantially accelerated at a chain length of $n = 6$ in tris(hydroxymethyl)aminomethane (Tris) buffer, whereas in borate and phosphate buffer no specificity was observed (Fig. 23). When the solvent composition was changed, namely, a 1 : 1 (v/v) methanol–water system was used, the substrate specificity in phosphate buffer was recovered for esters with $n = 10$–14 depending on catalyst concentration, whereas in Tris buffer it shifted to $n = 14$ and was constant at all polymer concentrations studied (Table 2).

The selectivity shifts were explained by changes in the morphology of the polymer aggregates, which can adsorb the substrates from methanol–water solution. A transition from spherical particles of **1** to rodlike and vesicle-like particles was suggested for phosphate buffer solutions. It was believed that the substrates with a definite tail length adsorb preferentially at the interfaces of the particles of the corresponding type (Table 2). Tris buffer was shown to increase the solubility of the polymer in the methanol–water mixture, which resulted in no morphological changes and, accordingly, changes in substrate specificity; the polymer aggregates were spherical in Tris buffer at all polymer concentrations studied.

Thus summarizing, the adsorption of substrate at the interfaces of polymer associates or emulsion droplets leads to the unusual effects associated with the progress of catalytic reactions in a nanoscale interfacial layer of the

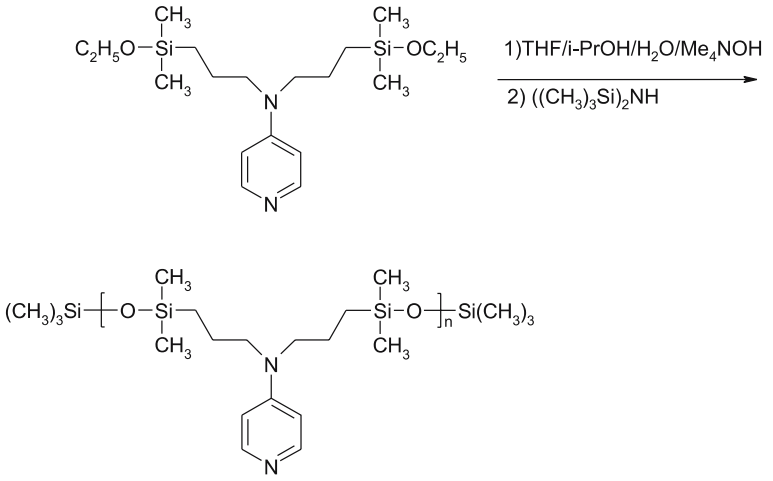

1

Scheme 8 Polycondensation of 4-[*N*,*N*-bis[(3-dimethylethoxysilyl)propyl]]aminopyridine

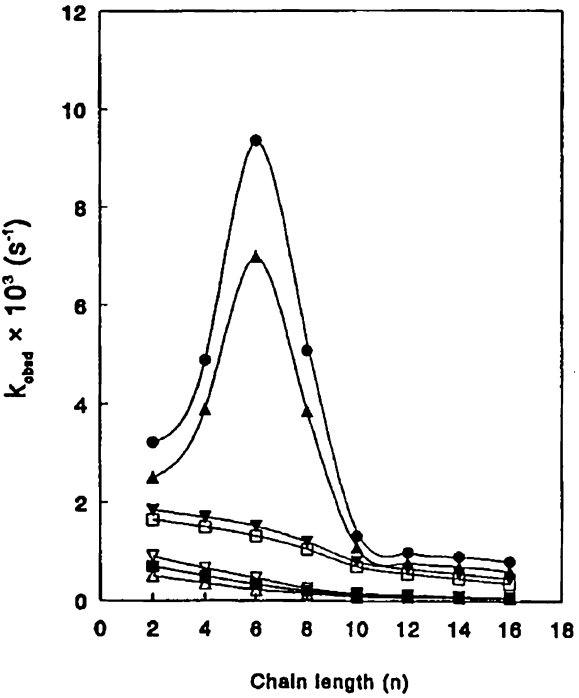

Fig. 23 Pseudo-first-order rate constants for the hydrolysis of NPAlk ($n = 2$–16) in the absence and in the presence of **1** as a function of alkanoate chain length n, catalyst concentration, and buffer system: *circles* 7.5×10^{-5} mol L^{-1} **1** in Tris(hydroxymethyl)aminomethane (*Tris*) buffer solution; *closed up triangles* 2.5×10^{-5} mol L^{-1} **1** in Tris buffer solution; *closed down triangles* 2.5×10^{-5} mol L^{-1} **1** in phosphate buffer solution; *open squares* 2.5×10^{-5} mol L^{-1} **1** in borate buffer solution; *open down triangles* in Tris buffer solution only; *closed squares* in phosphate buffer solution only; *open up triangles* in borate buffer solution only. (Reprinted with permission from [73]. Copyright 1996 American Chemical Society)

catalyst. It should be pointed out that interfacial reactions are of significant importance not only in catalytic applications. In biological systems, a great variety of interfaces between hydrophobic and hydrophilic areas are available, for example, in liposomes, cell membranes, and mitochondria. However, the role of interfaces is rarely taken into account in biophysical studies. Usually *n*-octanol–water partition coefficients are employed in many environmental and pharmacological studies to evaluate the allocation and fate of chemicals in environmental and biochemical systems. Partition coefficients characterize in a way the overall hydrophobicity of solutes. The latter appears to be one of the most important quantities since many binding sites of enzymes and receptors are quite susceptible to hydrophobic fragments of various low molecular weight compounds. However, as it is possible that reactions may proceed at the interface, the allocation of reacting compounds

Table 2 Substrate specificity [a] for **1**-catalyzed hydrolysis of *p*-nitrophenyl alkanoates (*NPAlk*) in 1 : 1 methanol–aqueous solution in the presence of polymer **1** aggregates. (Data from Ref. [76])

	Substrate specificity		Polymer aggregate morphology	
Concentration of **1** (mol/L)	Phosphate buffer (0.05 mol/L)	Tris buffer (0.05 mol/L)	Phosphate buffer (0.05 mol/L)	Tris buffer (0.05 mol/L)
5.0×10^{-6}	$n = 14$	$n = 14$	Sphere	Sphere
1.0×10^{-5}	$n = 14$	$n = 14$	Sphere	Sphere
2.5×10^{-5}	$n = 12$	$n = 14$	Rod	Sphere
5.0×10^{-5}	$n = 12$	$n = 14$	Rod	Sphere
7.5×10^{-5}	$n = 10$	$n = 14$	Vesicle	Sphere
1.0×10^{-4}	$n = 10$	$n = 14$	Vesicle	Sphere

Tris tris(hydroxymethyl)aminomethane

[a] Substrate specificity is defined by the maxima of plots of pseudo-first-order rate constants for the solvolysis of the series of the substrates as a function of NPAlk chain length *n*, see Fig. 23

in the interfacial areas should be taken into account, which was emphasized in a series of works [24, 25, 77, 78]. Goldar and Sikorav [77] studied the enhancement of renaturation of complementary single-stranded DNA in water–phenol emulsions. It was shown that adsorption of the DNA chains at water–phenol interfaces leads to a dramatic increase in the renaturation rate compared with the case of bulk solution. This was attributed both to the increase of the concentration of DNA strands at the interface and to a special conformation assumed by the strands upon interaction with the interfacial phenol molecules. It was stressed that knowledge of interfacial properties of molecules should be useful in understanding their biological properties. Adam and Delbruck [78] discussed the role of reduction of dimensionality in biological systems. They showed that in diffusion-controlled processes, the transition from three-dimensional to two-dimensional diffusion may result in an increase of the process rate. As an example, the take-up of pheromone molecules from air by developed surfaces of sense organs and further two-dimensional diffusion of the pheromone to target receptors was explored. Finally, along with their role in biological processes, the interfaces were suggested to promote significantly the evolution of living systems. In particular, Oparin [79] advanced a hypothesis that prebiotic reactions were taking place in heterogeneous, coacervated system; according to Onsager [80], oil–brine interfaces of the prebiotic environment might have been the first biochemical reactors (e.g., for interfacial polymerization). Thus, the aforementioned facts allow us to consider that polymer–water and oil–water interfaces are

a promising subject of research as media for chemical processes of a broad nature.

5 Conclusion

Recent studies showed that amphiphilic properties have to be taken into account for most water-soluble monomer units when their behavior in water solutions is considered. The amphiphilic properties of monomer units lead to an anisotropic shape of the polymer structures formed under appropriate conditions, which is confirmed both by computer simulation and experimental investigations. The concept of amphiphilicity applied to the monomer units leads to a new classification based on the interfacial and partitioning properties of the monomers. The classification in question opens a broad prospective for predicting properties of polymer systems with developed interfaces (i.e., micelles, polymer globules, fine dispersions of polymer aggregates). The relation between the standard free energy of adsorption and partition makes it possible to estimate semiquantitatively the distribution between the bulk and the interface of monomers and monomer units in complex polymer systems.

Amphiphilicity and surface activity of monomer units have a pronounced effect on self-organization in solutions of thermosensitive polymers. The balance of the hydrophilic and hydrophobic groups is markedly changed with the change of temperature. When the hydrophobic part prevails, a new stable microheterogeneous phase is formed with a definite size of aggregate particles [18, 81]. The possibility of obtaining nanostructures of interesting shape and behavior was shown for amphiphilic thermosensitive polymers when they were combined either with hydrophilic or hydrophobic moieties. Self-organization of thermosensitive polymers was shown to lead to formation of sharp water–polymer interfaces, which can act as catalytic *surface nanoreactors,* where chemical reactions take place with increased reaction rate, compared with the bulk solution. Two factors are responsible for that effect. First, the nanoreactors can adsorb and concentrate interfacially active substrates. Second, both substrate and catalyst moieties might be specifically oriented and subjected to additional high stress owing to the polymer concentration gradient. The adsorption of substrate at polymer–catalyst interfaces results in uncommon catalytic effects not only in the case of thermosensitive catalysts but also in the case of amphiphilic polymers of other types as well.

Finally, reactions in the *surface nanoreactors* were found to be important for biological objects such as DNA and pheromones; some hypotheses were advanced that the analogues of the surface nanoreactors might have played a significant role in biological evolution.

References

1. Vihola H, Laukkanen A, Hirvonen J, Tenhu H (2002) Eur J Pharm Sci 16:69
2. Murthy N, Campbell J, Fausto N, Hoffman AS, Stayton PS (2003) J Controlled Release 89:365
3. Twaites BR, de las Heras Alarcón C, Cunliffe D, Lavigne M, Pennadam S, Smith JR, Górecki DC, Alexander C (2004) J Controlled Release 97:551
4. Lim YB, Han SO, Kong HU (2000) Pharm Res 17:811
5. Lim Y, Choi YH, Park J (1999) J Am Chem Soc 121:5633
6. Bulmus V, Ding Z, Long CJ, Stayton PS, Hoffman AS (2000) Bioconjugate Chem 11:78
7. Hosoya K, Kubo T, Takahashi K, Ikegami T, Tanaka N (2002) J Chromatogr A 979:3
8. Gewehr M, Nakamura K, Ise N, Kitano H (1992) Makromol Chem 193:249
9. Kanazawa H, Yamamoto K, Matsushima Y, Takai N, Kikuchi A, Sakurai Y, Okano T (1996) Anal Chem 68:100
10. Kobayashi J, Kikuchi A, Sakai K, Okano T (2001) Anal Chem 73:2027
11. Kirsh YE, Vorobiev AV, Yanul NA, Fedotov YA, Timashev SF (2001) Sep Purif Technol 22–23:559
12. Hester JF, Olugebefola SC, Mayes AM (2002) J Membr Sci 208:375
13. Verspui GA, ten Brink GJ, Sheldon RA (1999) Chemtracts Org Chem 12:777
14. Franzen R, Xu Y (2005) Can J Chem Rev Can Chim 83:266
15. Cornils B, Herrmann WA (eds) (2004) Aqueous-phase organometallic catalysis: concepts and applications. 2nd edn. Wiley, New York
16. Haupt K, Mosbach K (2000) Chem Rev 100:2495
17. Wulff G (2002) Chem Rev 102:1
18. Okhapkin IM, Bronstein LM, Makhaeva EE, Matveeva VG, Sulman EM, Sulman MG, Khokhlov AR (2004) Macromolecules 37:7879
19. Rose GD, Geselowitz AR, Lesser GJ, Lee RH, Zehfus MH (1985) Science 229:834
20. Lau KF, Dill KA (1989) Macromolecules 22:3986
21. Lau KF, Dill KA (1990) Proc Natl Acad Sci USA 87:6388
22. Vasilevskaya VV, Khalatur PG, Khokhlov AR (2003) Macromolecules 36:10103
23. Vasilevskaya VV, Klochkov AA, Lazutin AA, Khalatur PG, Khokhlov AR (2004) Macromolecules 37:5444
24. Khokhlov AR, Okhapkin IM (2005) In: Adachi K, Sato T (eds) Structure and dynamics in macromolecular systems with specific interactions. Osaka University Press, Osaka, p 57
25. Okhapkin IM, Makhaeva EE, Khokhlov AR (2005) Colloid Polym Sci 284:117
26. Sangster J (1997) Octanol-water partition coefficients: fundamentals and physical chemistry. Wiley, Chichester
27. Kalizan R (1992) Anal Chem 64:619A
28. Griffin WC (1949) J Soc Cosmet Chem 1:311
29. Shih L-B, Mauer DH, Verbrugge CJ, Wu CF, Chang SL, Chen SH (1988) Macromolecules 21:3235
30. Wataoka I, Urakawa H, Kobayashi K, Akaike T, Schmidt M, Kajiwara K (1999) Macromolecules 32:1816
31. Thünemann AF, Wendler U, Jaeger W (2002) Langmuir 18:4500
32. Khokhlov AR, Khalatur PG (1998) Physica A 249:253
33. Khokhlov AR, Khalatur PG (1999) Phys Rev Lett 82:3456

34. Govorun EN, Ivanov VA, Khokhlov AR, Khalatur PG, Borovinsky AL, Grosberg AY (2001) Phys Rev E 64:040903
35. Kokufuta E (1993) Adv Polym Sci 110:157
36. Ben'Naim A (1982) In: Mittal KL, Fendler EJ (eds) Solution behaviour of surfactants: theoretical and applied aspects, vol 1. Plenum, New York, p 27
37. Makhaeva EE, Tenhu H, Khokhlov AR (1998) Macromolecules 31:6112
38. Makhaeva EE, Tenhu H, Khokhlov AR (2000) Polymer 41:9139
39. Rička J, Meewes M, Nyffenegger R, Binkert T (1990) Phys Rev Lett 65:657
40. Walter R, Ricka J, Quellet C, Nyffenegger R, Binkert T (1996) Macromolecules 29:4019
41. Wang X, Qiu X, Wu C (1998) Macromolecules 31:2972
42. Lau ACW, Wu C (1999) Macromolecules 32:58
43. Wang X, Wu C (1999) Macromolecules 32:4299
44. Qiu X, Wu C (1997) Macromolecules 30:7291
45. Virtanen J, Holappa S, Lemmetyinen H, Tenhu H (2002) Macromolecules 35:4763
46. Chen H, Li J, Ding Y, Zhang G, Zhang Q, Wu C (2005) Macromolecules 38:4403
47. Neradovic D, Soga O, Van Nostrum CF, Hennink WE (2004) Biomaterials 25:2619
48. Chen X, Ding X (2004) Colloid Polym Sci 283:452
49. Nuopponen M, Ojala J, Tenhu H (2004) Polymer 45:3643
50. Zhang G, Winnik FM, Wu C (2003) Phys Rev Lett 90:035506
51. Kim IS, Jeong YI, Cho CS, Kim SH (2000) Int J Pharm 211:1
52. Verbrugghe S, Laukkanen A, Aseyev V, Tenhu H, Winnik FM, Du Preza FE (2003) Polymer 44:6807
53. Vihola H, Laukkanen A, Valtola L, Tenhu H, Hirvonen J (2005) Biomaterials 26:3055
54. Bronstein LM, Kostylev M, Tsvetkova I, Tomaszewski J, Stein B, Makhaeva EE, Okhapkin I, Khokhlov AR (2005) Langmuir 21:2652
55. Liu XM, Yang YY, Leong KW (2003) J Colloid Interface Sci 266:295
56. Liu XM, Pramoda KP, Yang YY, Chow SY, He C (2004) Biomaterials 25:2619
57. Overberger CG, Corett R, Salarnone JC, Yaroslavsky S (1968) Macromolecules 1:331
58. Overberger CG, St Pierre T, Vorchheimer N, Lee J, Yaroslavsky S (1965) J Am Chem Soc 87:296
59. Kunitake T, Shimada F, Aso C (1969) J Am Chem Soc 91:2716
60. Kunitake T, Shinkai S (1971) J Am Chem Soc 93:4247
61. Kirsh YE, Kabanov VA, Kargin VA (1967) Dokl Akad Nauk 117:112
62. Starodubtsev SG, Kirsh YE, Kabanov VA (1974) Vysokomolek Soed A 16:2260
63. Yatsimirsky AK, Martinek K, Berezin IV (1971) Tetrahedron 27:2855
64. Berezin IV, Martinek K, Yatsimirsky AK (1973) Uspekhi Khimii 42:1729
65. Bobic C, Anghel FD, Voicu A (1995) Colloids Surf 105:305
66. Vriezema DM, Comellas Aragones M, Elemans JAAW, Cornelissen JJLM, Rowan AE, Nolte RJM (2005) Chem Rev 105:1445
67. Liu CY, Hu CC, Hung WH (1996) J Mol Catal 106:67
68. Ford WT (1997) React Funct Polym 48:3
69. Ford WT (2001) React Funct Polym 33:147
70. Vasilevskaya VV, Aerov AA, Khokhlov AR (2004) Dokl Phys Chem 398(6):1
71. Lawin LR, Fife WK, Tian CX (2000) Langmuir 16:3583
72. Guthrie JP (1973) Can J Chem 51:3494
73. Wang GJ, Ye D, Fife WK (1996) J Am Chem Soc 118:12536
74. Wang GJ, Fife WK (1997) Langmuir 13:3320
75. Wang GJ, Fife WK (1998) J Am Chem Soc 120:883

76. Wang GJ, Fife WK (1999) Macromolecules 32:559
77. Goldar A, Sikorav JL (2004) Eur Phys JE 14:211
78. Adam G, Delbruck M (1968) In: Rich A, Davidson N (eds) Structural chemistry and molecular biology. Freeman, San Francisco, p 198
79. Oparin AI (1965) Adv Enzymol 27:347
80. Onsager L (1974) In: Mintz SL, Widmayer SM (eds) Quantum statistical mechanics in the natural sciences. Plenum, New York, p 1
81. Laukkanen A, Valtola L, Winnik FM, Tenhu H (2004) Macromolecules 37:2268